

# Label-free second harmonic and hyper Rayleigh scattering with high efficiency

Nikolaos Gomopoulos, Cornelis Lütgebaucks, Qinchao Sun, Carlos Macias-Romero, and Sylvie Roke\*

Laboratory for fundamental BioPhotonics (LBP), Institute of Bio-engineering (IBI), School of Engineering (STI), Ecole Polytechnique Federale de Lausanne (EPFL), CH-1015 Lausanne, Switzerland  
\*sylvie.roke@epfl.ch

**Abstract:** We present a method to perform hyper Rayleigh scattering from aqueous solutions and second harmonic scattering measurements from unlabeled interfaces of liposomes and nanoparticles in dilute solutions. The water and interfacial response can be measured on a millisecond timescale, thus opening up the possibility to measure label-free time dependent transport processes in biological (membrane) systems.

©2013 Optical Society of America

OCIS codes: (240.3695) Optics at surfaces; (190.4350) Nonlinear optics.

---

## References and links

1. J. E. Rothman, "Mechanisms of intracellular protein transport," *Nature* **372**(6501), 55–63 (1994).
2. S. M. Butterfield and H. A. Lashuel, "Amyloidogenic Protein-Membrane Interactions: Mechanistic Insight from Model Systems," *Angew. Chem. Int. Ed. Engl.* **49**(33), 5628–5654 (2010).
3. D. S. Peterka, H. Takahashi, and R. Yuste, "Imaging Voltage in Neurons," *Neuron* **69**(1), 9–21 (2011).
4. T. F. Heinz, C. K. Chen, D. Ricard, and Y. Shen, "Spectroscopy of Molecular Monolayers by Resonant Second-Harmonic Generation," *Phys. Rev. Lett.* **48**(7), 478–481 (1982).
5. S. Roke, "Nonlinear optical spectroscopy of soft matter interfaces," *ChemPhysChem* **10**(9-10), 1380–1388 (2009).
6. R. W. Terhune, P. D. Maker, and C. M. Savage, "Measurements of nonlinear light scattering," *Phys. Rev. Lett.* **14**(17), 681–684 (1965).
7. R. Bersohn, Y. H. Pao, and H. L. Frisch, "Double-Quantum Light Scattering by Molecules," *J. Chem. Phys.* **45**(9), 3184–3198 (1966).
8. M. Kauranen and A. Persoons, "Theory of polarization measurements of second-order nonlinear light scattering," *J. Chem. Phys.* **104**(10), 3445–3456 (1996).
9. D. P. Shelton, "Polarization and angle dependence for hyper-Rayleigh scattering from local and nonlocal modes of isotropic fluids," *J. Opt. Soc. Am. B* **17**(12), 2032–2036 (2000).
10. D. P. Shelton, "Accurate hyper-Rayleigh scattering polarization measurements," *Rev. Sci. Instrum.* **82**(11), 113103 (2011).
11. K. Clays, M. J. Therien, and G. Hennrich, "Hyper-Rayleigh scattering for solution phase structure determination," *Linear and Nonlinear Optics of Organic Materials VIII* **7049** (2008).
12. S. Roke and G. Gonella, "Nonlinear Light Scattering and Spectroscopy of Particles and Droplets in Liquids," *Annu. Rev. Phys. Chem.* **63**(1), 353–378 (2012).
13. H. Wang, E. C. Y. Yan, E. Borguet, and K. B. Eisenthal, "Second harmonic generation from the surface of centrosymmetric particles in bulk solution," *Chem. Phys. Lett.* **259**(1-2), 15–20 (1996).
14. K. B. Eisenthal, "Second harmonic spectroscopy of aqueous nano- and microparticle interfaces," *Chem. Rev.* **106**(4), 1462–1477 (2006).
15. L. Schneider, H. J. Schmid, and W. Peukert, "Influence of particle size and concentration on the second-harmonic signal generated at colloidal surfaces," *Appl. Phys. B* **87**(2), 333–339 (2007).
16. S. Roke, W. G. Roeterdink, J. E. G. J. Wijnhoven, A. V. Petukhov, A. W. Kleyn, and M. Bonn, "Vibrational sum frequency scattering from a submicron suspension," *Phys. Rev. Lett.* **91**(25), 258302 (2003).
17. S. H. Jen, G. Gonella, and H. L. Dai, "The Effect of Particle Size in Second Harmonic Generation from the Surface of Spherical Colloidal Particles. I: Experimental Observations," *J. Phys. Chem. A* **113**(16), 4758–4762 (2009).
18. J. I. Dadap, J. Shan, and T. F. Heinz, "Theory of optical second-harmonic generation from a sphere of centrosymmetric material: small-particle limit," *J. Opt. Soc. Am. B* **21**(7), 1328–1347 (2004).
19. A. G. F. de Beer, S. Roke, and J. I. Dadap, "Theory of optical second-harmonic and sum-frequency scattering from arbitrarily shaped particles," *J. Opt. Soc. Am. B* **28**(6), 1374–1384 (2011).
20. G. Gonella and H. L. Dai, "Determination of adsorption geometry on spherical particles from nonlinear Mie theory analysis of surface second harmonic generation," *Phys. Rev. B* **84**(12), 121402 (2011).

21. H. Husu, R. Siikanen, J. Mäkitalo, J. Lehtolahti, J. Laukkanen, M. Kuittinen, and M. Kauranen, "Metamaterials with Tailored Nonlinear Optical Response," *Nano Lett.* **12**(2), 673–677 (2012).
22. J. Butet, I. Russier-Antoine, C. Jonin, N. Lascoux, E. Benichou, and P. F. Brevet, "Sensing with Multipolar Second Harmonic Generation from Spherical Metallic Nanoparticles," *Nano Lett.* **12**(3), 1697–1701 (2012).
23. Y. Liu, C. Y. Yan, X. L. Zhao, and K. B. Eisenthal, "Surface potential of charged liposomes determined by second harmonic generation," *Langmuir* **17**(7), 2063–2066 (2001).
24. M. Subir, J. Liu, and K. B. Eisenthal, "Protonation at the Aqueous Interface of Polymer Nanoparticles with Second Harmonic Generation," *J. Phys. Chem. C* **112**(40), 15809–15812 (2008).
25. B. Schürer, S. Wunderlich, C. Sauerbeck, U. Peschel, and W. Peukert, "Probing colloidal interfaces by angle-resolved second harmonic light scattering," *Phys. Rev. B* **82**(24), 241404 (2010).
26. S. Roke, J. Buitenhuis, J. C. van Miltenburg, M. Bonn, and A. van Blaaderen, "Interface-solvent effects during colloidal phase transitions," *J. Phys. Condens. Matter* **17**(45), S3469–S3479 (2005).
27. H. F. Wang, T. Troxler, A. G. Yeh, and H. L. Dai, "In Situ, Nonlinear Optical Probe of Surfactant Adsorption on the Surface of Microparticles in Colloids," *Langmuir* **16**(6), 2475–2481 (2000).
28. H. M. Eckenrode and H. L. Dai, "Nonlinear optical probe of biopolymer adsorption on colloidal particle surface: poly-L-lysine on polystyrene sulfate microspheres," *Langmuir* **20**(21), 9202–9209 (2004).
29. H. M. Eckenrode, S. H. Jen, J. Han, A. G. Yeh, and H. L. Dai, "Adsorption of a cationic dye molecule on polystyrene microspheres in colloids: Effect of surface charge and composition probed by second harmonic generation," *J. Phys. Chem. B* **109**(10), 4646–4653 (2005).
30. J. I. Dadap, X. Hu, N. Russell, J. Ekerdt, J. Lowell, and M. Downer, "Analysis of second-harmonic generation by unamplified, high-repetition-rate, ultrashort laser pulses at Si(001) interfaces," *IEEE J. Sel. Top. Quantum Electron.* **1**(4), 1145–1155 (1995).
31. Y. Wang, O. Zeiri, A. Neyman, F. Stellacci, and I. A. Weinstock, "Nucleation and Island Growth of Alkanethiolate Ligand Domains on Gold Nanoparticles," *ACS Nano* **6**(1), 629–640 (2012).
32. D. P. Shelton, "Slow polarization relaxation in water observed by hyper-Rayleigh scattering," *Phys. Rev. B* **72**(2), 020201 (2005).
33. L. Haber, S. J. J. Kwok, M. Semeraro, and K. B. Eisenthal, "Probing the colloidal gold nanoparticle/aqueous interface with second harmonic generation," *Chem. Phys. Lett.* **507**(1-3), 11–14 (2011).
34. J. Liu, M. Subir, K. Nguyen, and K. B. Eisenthal, "Second Harmonic Studies of Ions Crossing Liposome Membranes in Real Time," *J. Phys. Chem. B* **112**(48), 15263–15266 (2008).
35. *Handbook of Biomedical Nonlinear Optical Microscopy* (Oxford University Press, Oxford, 2008).
36. K. Kuetemeyer, R. Rezgui, H. Lubatschowski, and A. Heisterkamp, "Influence of laser parameters and staining on femtosecond laser-based intracellular nanosurgery," *Biomed. Opt. Express* **1**(2), 587–597 (2010).
37. D. O. Lapotko and E. Y. Lukianova, "Influence of Physiological Conditions on Laser Damage Thresholds for Blood, Heart, and Liver Cells," *Lasers Surg. Med.* **36**(1), 13–21 (2005).
38. K. König, "Multiphoton microscopy in life sciences," *J. Microsc.* **200**(2), 83–104 (2000).
39. A. Vogel, N. Linz, S. Freidank, and G. Paltauf, "Femtosecond-Laser-Induced Nanocavitation in Water: Implications for Optical Breakdown Threshold and Cell Surgery," *Phys. Rev. Lett.* **100**(3), 038102 (2008).
40. D. J. Payne, R. A. Hopkins, B. G. Eilert, G. D. Noojin, D. J. Stolarski, R. J. Thomas, C. P. Cain, G. T. Hengst, P. K. Kennedy, T. R. Jost, and B. A. Rockwell, "Comparative Study of Laser Damage Threshold Energies in the Artificial Retina," *J. Biomed. Opt.* **4**(3), 337–344 (1999).

## 1. Introduction

Many biological and chemical properties that involve nano- and micron-sized objects, like colloids, micelles, viruses, liposomes and living cells are depending on processes occurring at the object/medium interface. Examples include transport of proteins and reagents through membranes, uptake of oxygen in blood cells, formation of fibrous plaques related to Alzheimer's disease, and electrostatic current flow through the outer membrane of dendrites and axons of neural cells [1–3]. Such processes are usually confined to a 1 nm thin layer that surrounds the object. In addition they exhibit fast kinetics in the (sub)-ms regime.

Second-order nonlinear optical techniques are sensitive to non-centrosymmetry as the second-order susceptibility vanishes in isotropic bulk media (in the electric dipole approximation). Second harmonic (SHG) and sum frequency (SFG) generation have therefore become valuable tools for studying interfacial properties [4, 5]. SHG and SFG have also shown to be applicable as light scattering techniques (termed hyper Rayleigh scattering (HRS), second harmonic scattering, (SHS) and sum frequency scattering, (SFS)). HRS is an incoherent light scattering technique that originates from local density/orientational fluctuations that exist in any medium on the time scale of the laser pulse. The HRS response is very weak for gases and liquids and it is mostly used to characterize the incoherent nonlinear optical response of molecules (usually chromophores) [6–11]. Although HRS and SHS both

depend on the generation and detection of SH photons, we choose to use different names to differentiate between the incoherent (HRS) and coherent nature (SHS) of both methods [12]. SHS and SFS are used to measure the interfacial properties of nanoscopic particles, droplets, and vesicles in liquid and solid matrices [13–17]. In an SHS experiment a femtosecond pulsed laser beam is focused into a sample cell or a jet containing droplets or particles. The scattered SH light is emitted in a typical scattering pattern from which the surface properties can be deduced [18–20]. Being able to detect interfacial properties from nanoparticles in solution or otherwise arranged in three dimensional space offers great opportunities for designing nanomaterials, biosensors, and metamaterials [21, 22].

Both SH and SF scattering are candidates for label-free detection of kinetics, self-assembly, and transport processes in biological systems on the ms timescale. Indeed, SFs and SHS have been used label-free to detect structural changes, and electrostatic potentials [23–26], but time dependent (kinetics) measurements have been performed using the help of a marker with a resonance at the SH frequency [27–29]. This is caused by the relatively low efficiency of the off-resonant interface selective SHG and SFG processes.

Here, we employ an optical scheme for SHS, which is optimized for label-free detection. Since the SH efficiency scales linearly with repetition rate but quadratically with the pulse energy a high detection efficiency can be expected [30]. We show this indeed to be the case. First we perform experiments on polystyrene (PS) beads in aqueous solution to ensure that the surface response of the PS particle is measured. This is followed by HRS measurements on water, which can be used as a benchmark for comparing our detection efficiency to earlier published results. Finally we show scattering results for PS particles, liposomes and Au nanoparticles and compare the relative scattering efficiency.

## 2. Experiments and results

The experiments were performed using a pulsed Yb:KGW femtosecond laser system (Light Conversion Ltd) delivering 190 fs pulses centered at 1028 nm with a 200 kHz repetition rate. The selectively polarized pulses were focused into a cylindrical glass sample cell (4 mm optical path length (Scott)) down to a  $\sim 50$   $\mu\text{m}$  beam waist. The scattered light was then collimated with a lens, polarization selected and spectrally dispersed onto an intensified charge coupled device (CCD) camera (PiMax 3, Princeton Instruments). The angle of acceptance was controlled by an aperture placed in front of the collimating lens and was controlled between 1 and 5°. Filters were used to separate the SH photons from the fundamental and any background signal. Figure 1 illustrates the optical layout of the experimental setup. Unless specified otherwise, the power was kept at 118 mW as measured before the sample. The SH intensity ( $I_{\text{SH}}$ ) was measured from the aqueous particle solutions as well as the HRS signal ( $I_{\text{HRS}}$ ) from the (particle free) aqueous solutions. The surface SH response ( $I_{\text{SHS,PP}} - I_{\text{HRS,PP}}$ ) was normalized by the HRS intensity from water:  $(I_{\text{SHS,PP}} - I_{\text{HRS,PP}}) / I_{\text{HRS,SS}}$  [25]. The polarization combination for the SHS was PP, which is most sensitive to the interfacial structure. The interfacial response is obtained by subtracting the response from the particle free solution in the same polarization combination. We normalized that signal with the SS response of the water, which is angle independent and the strongest response for the HRS process. P refers to horizontally and S refers to vertically polarized light.

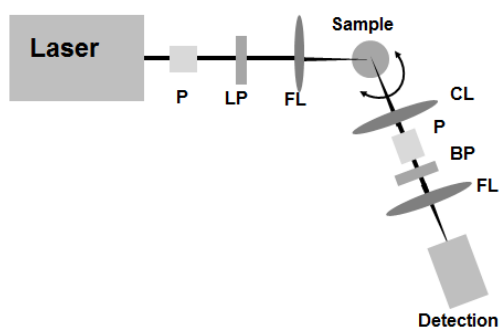


Fig. 1. Optical setup used for SH scattering measurements. P: Polarizer, LP: long pass filter, FL: focusing lens, CL: Collimating lens, BP: band pass filter. The detection arm can be adjusted to any orientation from  $-120^\circ$  to  $120^\circ$ .

PS nanoparticles (Polysciences.Inc) with a diameter of 500 nm were used. The surface of the particles carried a negative charge due to the presence of sulfate groups. The PS beads were used as received and dispersed in aqueous solution with a fixed concentration of 0.026 v.v%. 1-palmitoyl-2-oleoyl-*sn*-glycero-3-phospho-(1'-*rac*-glycerol) (POPG, Avanti polar lipids, INC) liposomes were prepared by evaporating a 12.5 mg/ml solution of POPG in chloroform under vacuum for more than 4 hrs. The resulted film was hydrated by adding PBS buffer. POPG vesicles were then formed by extrusion through 100 nm polycarbonate film at room temperature and the liposome solution was diluted 40 times for the SHG measurement. The Au nanoparticles contained 12  $\mu\text{g/ml}$  of particles with an average diameter of 8 nm and were provided by Randy Patrick Garney and Prof. Francesco Stellacci [31]. The aqueous solutions were prepared with ultrapure 18 M $\Omega$  water.

To prove that the observed signal originates from the surface of the particles and not from non-linear bulk processes, we performed a number of experiments. First, by varying the focus of the incident beam and using sample cells of different optical path lengths, it was shown that the SH light did not originate from either the input or output windows of the cells. This was further verified by using a liquid jet produced in a pump driven flow system as in Ref [17]. Second, we examined the spectrum of the SH signal and verified that the SH spectrum appears exactly at the double frequency and has the pulse limited width. By placing a  $\beta$ -BBO crystal in the fundamental beam and recording the spectrum, we observed that the SHS spectrum was identical to the generated SH spectrum.

Figure 2 displays two further characteristics of SH scattering: a quadratic dependence on the laser pulse intensity and a linear dependence on the particle density. Figure 2(a) highlights this behavior, for the case of an aqueous solution of 500 nm diameter PS particles. Finally, in order to probe the incoherent nature of the scattering process, we investigated the dependence of the SH intensity on the density of scatterers in solution. Figure 2(b) illustrates the obtained results for aqueous solution of 500 nm PS particles over a range of particles densities of  $1-10 \times 10^9 / \text{cm}^3$ . The observed linear dependence indicates that the nano-particles do not exhibit coherent interactions. If this was the case, a nonlinear dependence of the SH signal on particle density would be the result [15]. The same linear dependence is observed for the liposomes and the gold nanoparticles.

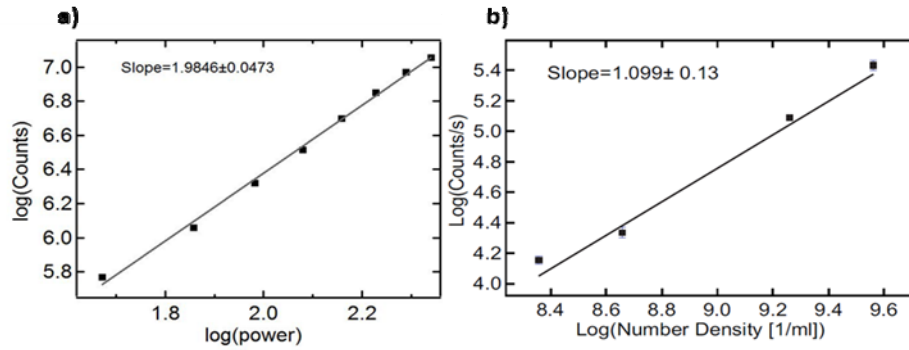


Fig. 2. a) The power dependence in PP polarization of SHS from a 0.026 v.v. % solution of PS beads. The power was measured in mW before the focus. The scattered light was detected at  $30^\circ$  degrees with an angle of acceptance of  $2^\circ$  and 10 s acquisition time. (b) SH intensity as a function of particle density from aqueous solutions of PS particles with a diameter of 500 nm, recorded under the same experimental condition as in a. The best fit solid line indicates a linear dependence.

To compare the detection efficiency and signal to noise ratio, we compared experimental parameters and results from the literature [13, 17, 25, 32]. As a reference we used the HRS signal of water [25]. We then compared the performance of the newly developed setup with the experimental results of Ref [25], which reports, as far as we are aware, the best detection efficiency and highest signal to noise ratio. In this study the scattering signal from PS beads in water is given as well as the angular independent HRS signal of water. We used the same power and a detection angle of  $90^\circ$  and compared our acquisition time for the HRS measurements in SS polarization. Figure 3 shows HRS data measured with different acquisition times. It can be seen that a signal can be measured down to the millisecond time range. The inset shows the retrieved spectral response for 5 ms (1000 pulses). An acquisition time of 1 ms is 500 times shorter than what is reported in [25]. We also found that the system proposed here is shot-noise limited. We anticipate that if the ultralow response of water can be measured with 1 ms time resolution, then the stronger response of interfaces can be recorded on timescales that are important for biological processes.

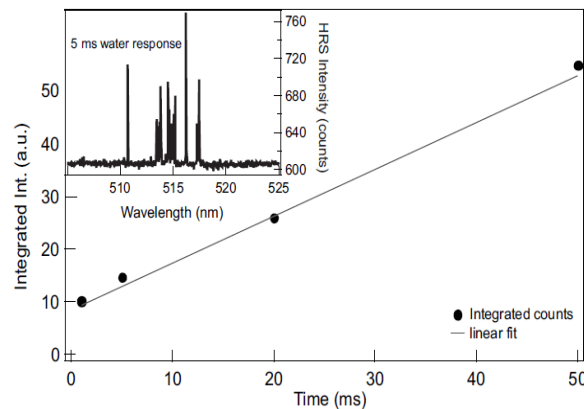


Fig. 3. HRS intensity from pure water as a function of acquisition time. The inset shows the response for a time lapse of 5 ms (1000 laser shots). The angular resolution was  $5^\circ$  degrees and the scattering angle was set at  $90^\circ$ .

Finally we investigated the dependence of the SH intensity on the surface response of three different materials. Spectra of 500 nm diameter PS particles in water and 8 nm Au nanoparticles are shown in Fig. 4(a). The polystyrene intensity reflects the exact SH spectral response of the pulse, while the Au nanoparticles exhibit a broader spectrum. The broadening is due to excitation of the plasmon resonance. Note that we have subtracted the fluorescence that is present as a broad background. The liposome spectrum has the same shape as the polystyrene spectrum and is therefore not shown. The signal strength for three different samples is shown in Fig. 4(b), where Au nanoparticles and polystyrene beads are compared with 100 nm liposomes (composed of POPG).

Comparison of our findings to literature (polystyrene [25], Au nanoparticles [33], and liposomes [23, 34]) suggests a marked increase in the performance of the proposed optical configuration. The reason for this relative increase in performance probably lies in the range of pulse energies used in combination with gated detection. While our instrument runs at similar or lower power as [13, 17, 25, 32], we are able to obtain higher signals because the SH intensity scales quadratically with the pulse energy. When using high efficiency chromophores our optical layout is relatively inefficient since the optical response of the chromophores saturates at much lower pulse energies. Therefore, the optimum laser sources for chromophore experiments (such as two photon spectroscopy or SH microscopy) are those that deliver  $\sim 1$  nJ of pulse energy at a high repetition rate ( $\sim 90$  MHz) [35]. For unstained biological systems it has been shown that the damage threshold for pulse energies is much higher [36–40]. Furthermore in going from nJ pulses delivered by high repetition rate sources to  $\mu$ J pulse energies delivered in the kHz regime the damage mechanism changes from electron induced chemical decomposition to plasma mediated nano-cavities [39]. Thus for label free experiments the proposed geometry appears to be extremely efficient and it can easily be extended towards microscopy.

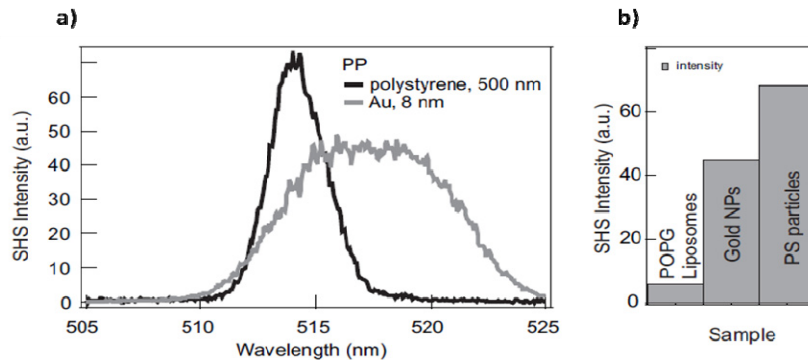


Fig. 4. a) SHS spectra recorded (at a detection angle of  $30^\circ$ ) from the surface of PS particles in water (0.026 v.v%, 500 nm diameter), and 8 nm gold nanoparticles in water. The SHS spectrum of the PS beads follows the shape of the frequency doubled laser spectrum, while the spectral response from the Au nanoparticles is broadened by the resonance of the SH light with the 520 nm centered plasmon resonance. b) Comparison of signal strengths for liposomes (100 nm, 0.075 v.v %), nanoparticles (8 nm, 12  $\mu$ g/ml), and polystyrene particles (500 nm, 0.026 v.v %).

### 3. Conclusions

In summary, we have presented a method to perform label-free SHS experiments with a high efficiency and millisecond detection time. We can obtain interfacial responses from dilute suspensions of nanoparticles and liposomes as well as HRS from water on the millisecond timescale. The pulse peak powers and fluencies used are well below the threshold for optical damage of aqueous systems and living cells ( $\sim 0.5 - 1$  TW/cm<sup>2</sup> [36, 37, 39]). Therefore, nonlinear light scattering (or microscopy) experiments using this type of optical layout can be used to probe kinetic interfacial processes in biological systems label free.

## **Acknowledgments**

This work is supported by the Julia Jacobi Foundation, the Swiss National Foundation (grant number 200021\_140472), and the European Research Council (grant number 240556). We would like to thank Randy Patrick Garney and Prof. Francesco Stellacci for kindly synthesizing and providing the Au nanoparticles.